Quantum fractals in boxes

1996 J. Phys. A: Math. Gen. 29 6617

(http://iopscience.iop.org/0305-4470/29/20/016)

J. Phys. A: Math. Gen. **29** (1996) 6617–6629. Printed in the UK

Quantum fractals in boxes

M V Berry
H H Wills Physics Laboratory, Tyndall Avenue, Bristol BS8 1TL, UK

Received 22 April 1996

Abstract. A quantum wave with probability density $P(\boldsymbol{r}, t) = |\Psi(\boldsymbol{r}, t)|^2$, confined by Dirichlet boundary conditions in a D-dimensional box of arbitrary shape and finite surface area, evolves from the uniform state $\Psi(\boldsymbol{r}, 0) = 1$. For almost all positions $\boldsymbol{r} = x_1, x_2 \ldots x_D$, the graph of the evolution of P is a fractal curve with dimension $D_{\text{time}} = 7/4$. For almost all times t, the graph of the spatial probability density P is a fractal hypersurface with dimension $D_{\text{space}} = D + 1/2$. When $D = 1$, there are, in addition to these generic time and space fractals, infinitely many special 'quantum revival' times when P is piecewise constant, and infinitely many special spacetime slices for which the dimension of P is 5/4. If the surface of the box is a fractal with dimension $D - 1 + \gamma$ $(0 \leqslant \gamma < 1)$, simple arguments suggest that the dimension of the time fractal is $D_{\text{time}} = (7 + \gamma)/4$, and that of the space fractal is $D_{\text{space}} = D + 1/2 + \gamma/2$.

1. Introduction

My purpose here is to draw attention to some unexpected fractal properties of the probability density

$$P(\boldsymbol{r}, t) \equiv |\Psi(\boldsymbol{r}, t)|^2 \qquad (\boldsymbol{r} = \{x_1, x_2, \ldots x_D\}) \tag{1}$$

for what is perhaps the simplest imaginable nonstationary Schrödinger wave Ψ. This evolves from a spatially uniform initial state in a D-dimensional box B, confined by Dirichlet boundary conditions at the impenetrable walls ∂B, that is, in appropriate units,

$$\begin{aligned} &\mathrm{i}\partial_t \Psi(\boldsymbol{r}, t) = -\nabla^2 \Psi(\boldsymbol{r}, t); \\ &\Psi(\boldsymbol{r}, t) = 0 \text{ for } \boldsymbol{r} \text{ on } \partial B; \qquad \Psi(r, 0) = 1 \text{ for } \boldsymbol{r} \text{ in } B. \end{aligned} \tag{2}$$

Ψ is a superposition of the modes $\phi_n(\boldsymbol{r})$ of the box; these satisfy

$$\begin{aligned} &-\nabla^2 \phi_n(\boldsymbol{r}) = k_n^2 \phi_n(\boldsymbol{r}), \\ &\phi_n(\boldsymbol{r}) = 0 \text{ for } \boldsymbol{r} \text{ on } \partial B, \qquad \int_B \mathrm{d}^D\boldsymbol{r}\, \phi_n^2(\boldsymbol{r}) = 1. \end{aligned} \tag{3}$$

The solution of (2) is

$$\Psi(\boldsymbol{r}, t) = \sum_{n=0}^{\infty} c_n \phi_n(\boldsymbol{r}) \exp\left\{-\mathrm{i}k_n^2 t\right\}, \qquad \text{where } c_n = \int_B \mathrm{d}^D\boldsymbol{r}'\, \phi_n(\boldsymbol{r}') \tag{4}$$

In (2) the initial and boundary conditions are discordant, enforcing an initial discontinuity at the walls. As I shall show, the effect of this discontinuity is to make the superposition $\Psi(\boldsymbol{r}, t)$ a fractal function in time and space. The fractality of Ψ depends on the high eigenstates $n \to \infty$ in the superposition, that is, on the semiclassical asymptotics of the wave. Nevertheless, the fractal dimensions of the time fractals (section 2) and the

0305-4470/96/206617+13\$19.50

space fractals (section 3) are universal, that is independent of the chaos or integrability of the geodesics in the box, provided the ($D - 1$-dimensional) area of ∂B is finite. In section 4 the special case of a one-dimensional box is studied in detail, and the fractal properties illustrated by computations. The general arguments do not apply to boxes with fractal boundaries, for which the area of ∂B is infinite; these are considered in section 5.

The same fractal properties in time and space will apply to any boundary condition except Neumann (for which the spatially uniform wave persists, because it is an eigenstate), and to any initial state with a spatial discontinuity anywhere. Although all these fractals are exact solutions of the Schrödinger equation in boxes, they represent states with infinite energy, so that any physical implementation can only be approximate: the finest fractal detail will be softened in a way that depends on the largest n (highest energy k_n^2) in the superposition. Nevertheless, the analogues of the time and space fractals have been seen in the optical Talbot effect (Berry and Klein 1996), in transverse and longitudinal sections of the field beyond a coherently-illuminated diffraction grating (these optical fractals are not exact solutions of Maxwell's equations, and their fine detail is softened by non-paraxial effects).

More generally, I expect time and space fractals to develop from discontinuous initial states in quantum systems that are not billiards—for example smooth potentials—and, more generally still, for any linear wave equation with a nonlinear dispersion relation; calculation of the fractal dimensions in any such case should be a simple extension of the methods presented here.

The calculations of fractal dimensions (Mandelbrot 1982) will depend on the application to Ψ of a result for Fourier series

$$f(u) = \sum_m a_m \exp\{\mathrm{i}mu\} \tag{5}$$

where a_m have random or pseudorandom phases. If the power spectrum $|a_m|^2$ has the asymptotic form

$$|a_m|^2 \sim |m|^{-\beta} \qquad \text{as } |m| \to \infty, \text{ where } 1 < \beta \leqslant 3, \tag{6}$$

then the graphs of $\operatorname{Re} f$ and $\operatorname{Im} f$ are continuous but non-differentiable, with fractal dimension

$$D_f = \tfrac{1}{2}(5 - \beta). \tag{7}$$

Thus $\beta = 3$ corresponds to a (just) differentiable curve with $D_f = 1$, and $\beta = 1$ would correspond to an area-filling curve with $D_f = 2$. Equation (7) can be obtained (by simple dimensional analysis) from the result (Orey 1970) that if f has dimension D_f the mean square increment of $f(u)$ over an infinitesimal distance Δu is proportional to $(\Delta u)^{4-2D_f}$; for a straightforward derivation (see Berry and Lewis 1980). This applies when D_f represents the capacity dimension, but in the present context I expect it to hold for the Hausdorff and other fractal dimensions as well.

Almost always, the graph of $|f(u)|^2$ also has the fractal dimension D_f. This follows from two facts: for real functions, squaring corresponds to local multiplication by a constant (e.g. in the interval $\operatorname{Re} f$ to $\operatorname{Re} f + \Delta$, Δ expands to $2\Delta \operatorname{Re} f$), which leaves the fractal dimension invariant; and fractal dimension is preserved in the sum $(\operatorname{Re} f(u))^2 + (\operatorname{Im} f(u))^2$, unless $\operatorname{Re} f$ and $\operatorname{Im} f$ are too closely connected (for example if the fractality of f is embodied in a phase factor). The appendix contains a direct demonstration from (5) and (6) that $|f(u)|^2$ has the dimension D_f. Therefore the fractal properties of $\operatorname{Re}\Psi$ and $\operatorname{Im}\Psi$ are inherited by the probability density $P(\boldsymbol{r}, t)$.

2. Time fractals

Consider the wave (4) as a function of t for fixed $\boldsymbol{r}$. To apply (7), the power spectrum in the mode label n must be transformed into that for the Fourier variable $k_n^2 \equiv E$ (E is the analogue of m in (5)). Thus the power spectrum is

$$|a(E)|^2 = |c_n|^2 \, \phi_n^2(\boldsymbol{r}) \frac{\mathrm{d}n}{\mathrm{d}E}. \tag{8}$$

From the Weyl rule for quantum billiards (Baltes and Hilf 1976),

$$n(E) \approx CVE^{D/2} \tag{9}$$

where V is the volume of B, and here and hereafter C will denote a generic dimensionless constant. The formula (8) should be interpreted as an average over many states with quantum numbers near $n(E)$. Normalization fixes the average of $\phi_n^2(\boldsymbol{r})$ as $1/V$ for all $\boldsymbol{r}$, so that

$$|a(E)|^2 = c_n^2 C E^{D/2-1}. \tag{10}$$

The mode coefficient c_n is given by (4), (3) and the divergence theorem as

$$c_n = -\frac{1}{E}\int_B \mathrm{d}^D\boldsymbol{r}\, \nabla^2 \phi_n(\boldsymbol{r}) = -\frac{1}{E}\int_{\partial B} \mathrm{d}^{D-1}\boldsymbol{r}\, \partial_{\mathrm{out}}\phi_n(\boldsymbol{r}) \tag{11}$$

where ∂_{out} denotes the outward normal derivative. Recalling that the fractal dimension depends on the semiclassical asymptotics, that is large n, we can calculate the boundary integral in (11) locally, by representing ϕ_n as the superposition of Dirichlet-adapted plane waves. If z is the inward normal coordinate, $\boldsymbol{u} = \{u_1, \ldots u_{D-1}\}$ are coordinates on ∂B, and there are N waves in the superposition, then

$$\phi_n(\boldsymbol{r}) = \frac{C}{\sqrt{NV}} \sum_{\boldsymbol{k}} \sin\{k_z z\} \cos\{\boldsymbol{k_u}\cdot\boldsymbol{u} + \alpha_{\boldsymbol{k}}\}, \qquad \text{where } k_z^2 + |\boldsymbol{k_u}|^2 = E \tag{12}$$

where the $\alpha_{\boldsymbol{k}}$ are sets of phases, different for each state n. Thus

$$\partial_{\mathrm{out}}\phi_n(\boldsymbol{u}, 0) = -\frac{C}{\sqrt{NV}} \sum_{\boldsymbol{k}} k_z \cos\{\boldsymbol{k_u}\cdot\boldsymbol{u} + \alpha_k\}. \tag{13}$$

Inserting this expression into (11) and averaging over the phases of states near E, we find

$$c_n^2 = \frac{CA}{VE^2} \int \mathrm{d}^{D-1}\boldsymbol{v} \left\langle k_z^2 \cos\{\boldsymbol{k_u}\cdot\boldsymbol{v}\}\right\rangle = \frac{CA}{VE} \left\langle \delta(\boldsymbol{k_u})\right\rangle \tag{14}$$

where A is the area of ∂B and $\langle\,\rangle$ denotes averages over the distribution of wavevectors $\boldsymbol{k}$. The semiclassical limit for groups of states dictates that the density $\mathrm{prob}(\boldsymbol{k})$ must be microcanonical, that is

$$\mathrm{prob}(\boldsymbol{k}) = \frac{\delta(E - k^2)}{\int \mathrm{d}^D\boldsymbol{k}\, \delta(E - k^2)}. \tag{15}$$

Elementary scaling gives

$$\langle\delta(\boldsymbol{k_u})\rangle = \frac{\int \mathrm{d}k_z\, \mathrm{d}^{D-1}\boldsymbol{k_u}\, \delta\left(E - k_z^2 - |\boldsymbol{k_u}|^2\right)\delta(\boldsymbol{k_u})}{\int \mathrm{d}^D\boldsymbol{k}\, \delta(E - k^2)} = \frac{C}{E^{(D-1)/2}} \tag{16}$$

and thence, from (14), the mode coefficient

$$c_n^2 = \frac{CA}{VE^{(D+1)/2}}. \tag{17}$$

The same result can be guessed directly from the boundary integral (11), using the principle that the normal derivative on ∂B consists of randomly positive and negative peaks whose linear dimensions are approximately the wavelength $1/k$ corresponding to E, and whose heights are of order k. Thus $c_n \sim (1/E) \times k \times$ (area of peak $= k^{-(D-1)}) \times \sqrt{(\text{number of peaks} = Ak^{(D-1)})} \sim E^{-(D+1)/4}$.

Thus the power spectrum (10) is

$$|a(E)|^2 = \frac{CA}{VE^{3/2}}. \tag{18}$$

Now we can identify $\beta = 3/2$ in (6) and hence, from (7), the fractal dimension of the evolution of the probability density

$$D_{\text{time}} = \frac{7}{4}. \tag{19}$$

This is the main result of this section.

The foregoing argument involved groups of states, rather than individual states, and so applies to all boxes, independently of their classical integrability. However, the emphasis on microcanonical averaging is reminiscent of classical chaos (Berry 1977), and so it is interesting and instructive to obtain the power spectrum (18) explicitly for two integrable boxes, using different arguments.

The first box is the D-dimensional cube of side L. The states, labelled by the vector of quantum numbers $\boldsymbol{n} = \{n_1, n_2, ...n_D\}$, are

$$\phi_{\boldsymbol{n}}(\boldsymbol{r}) = \left(\frac{2}{L}\right)^{D/2} \prod_{s=1}^{D} \sin\left(\frac{\pi n_s x_s}{L}\right). \tag{20}$$

Integration over the box eliminates the states with even quantum numbers, so we can label the states with the reduced set

$$\boldsymbol{q} = \{q_1, q_2, \ldots q_D\}, \qquad (0 \leqslant q_s \leqslant \infty), \qquad \text{where } n_s \equiv 2q_s + 1. \tag{21}$$

Thus

$$c_{\boldsymbol{q}}^2 = \left(\frac{2L}{\pi^2}\right)^D \prod_{s=1}^{D} \frac{1}{\left(q_s + \frac{1}{2}\right)^2}. \tag{22}$$

The energy is

$$E(\boldsymbol{q}) = k_{\boldsymbol{q}}^2 = \left(\frac{2\pi}{L}\right)^2 \sum_{s=1}^{D} \left(q_s + \tfrac{1}{2}\right)^2 \tag{23}$$

and the power spectrum, obtained from the analogue of (8), is

$$|a(E)|^2 = \frac{1}{L^D} \sum_{\boldsymbol{q}} c_{\boldsymbol{q}}^2 \, \delta\{E - E(\boldsymbol{q})\}. \tag{24}$$

In finding the asymptotics of this expression for large E, the simplest strategy, of replacing the sum by an integral, fails because it leads to a divergence. This is because the main contributions come from the neighbourhood of the coordinate axes in $\boldsymbol{q}$ space. Integrating along each axis, and summing perpendicularly, gives

$$|a(E)|^2 \approx \frac{DL^2}{4\pi^2} \left(\frac{2}{\pi^2}\right)^D \int_0^\infty \frac{\mathrm{d}q_1}{q_1^2} \sum_{q_2,\ldots q_D} \prod_{s=2}^{D} \frac{1}{\left(q_s + \frac{1}{2}\right)^2} \delta\left\{\left(\frac{L}{2\pi}\right)^2 E - q_1^2 - \sum_{s=2}^{D} \left(q_s + \tfrac{1}{2}\right)^2\right\}$$

$$= \frac{D\pi}{8L\,E^{3/2}}\left(\frac{2}{\pi^2}\right)^D \sum_{q_2,\ldots q_D}\prod_{s=2}^{D} \frac{1}{\left(q_s+\frac{1}{2}\right)^2\left[1-\frac{4\pi^2}{L^2E}\sum_{s=2}^{D}\left(q_s+\frac{1}{2}\right)^2\right]^{3/2}}$$

$$\approx \frac{D\pi}{8L\,E^{3/2}}\left(\frac{2}{\pi^2}\right)^D \sum_{q=0}^{\infty}\frac{1}{\left(q+\frac{1}{2}\right)^2} = \frac{D}{2^{D+1}\pi\,L\,E^{3/2}} \tag{25}$$

in agreement with the general result (18).

The second box is the unit disc in the plane. In polar coordinates $\boldsymbol{r} = (r, \theta)$, the modes are

$$\phi_{nl}(\boldsymbol{r}) = N_{nl}\,J_l(r\,j_{nl})\exp\{i\ l\theta\}\,, \qquad E_{nl} = k_{nl}^2 = j_{nl}^2 \tag{26}$$

where j_{nl} is the nth zero of the Bessel function J_l, and N_{ln} are normalization constants. Integration over the disk eliminates the states with $l \neq 0$, leaving (after normalization)

$$c_n = -\frac{2\sqrt{\pi}}{j_{n0}}. \tag{27}$$

Thus the states selected by the superposition are those with no variation round the boundary of the disk; this is analogous to the factor $\delta(\boldsymbol{k_u})$ in the general equation (14), which also locally eliminates variations on ∂B. For large n, $j_{n0} \approx \pi(n - 1/4)$. The power spectrum is therefore

$$|a_n|^2 = \frac{4\pi}{j_{n0}^2}\,\frac{1}{\pi}\,\frac{\mathrm{d}n}{\mathrm{d}E} \approx \frac{2}{\pi\,E^{3/2}} \tag{28}$$

again agreeing with the general result (18).

3. Space fractals

Considered as a function of $\boldsymbol{r}$, the graph of the probability density $P(\boldsymbol{r}, t)$ is a hypersurface, whose fractal dimension D_{space}, between D and $D+1$, we now determine. From the superposition (4), the momentum (i.e. wavevector) probability density is

$$\left|\bar{\Psi}(\boldsymbol{p})\right|^2 = \sum_m\sum_n c_m c_n \bar{\phi}_n^*(\boldsymbol{p})\bar{\phi}_m(\boldsymbol{p})\exp\left\{\mathrm{i}(k_m^2 - k_n^2)t\right\} \tag{29}$$

where the overbars denote Fourier transforms. Slight averaging over $\boldsymbol{p}$ or t (regarding the exponentials as pseudorandom phases) diagonalizes the double sum, giving the spatial power spectrum as

$$\left|\bar{\Psi}(\boldsymbol{p})\right|^2 = \sum_n c_n^2\left|\bar{\phi}_n(\boldsymbol{p})\right|^2. \tag{30}$$

For the large n and p that determine the spatial fractality, we can use (17) for the mode coefficients, and the semiclassical microcanonical momentum distribution (15) for the eigenmodes, so that

$$\left|\bar{\Psi}(\boldsymbol{p})\right|^2 \approx \sum_n c_n^2\frac{\delta(p - k_n)}{\int \mathrm{d}^D\boldsymbol{p}'\,\delta\left(p' - k_n\right)} \approx C\left[\frac{c_n^2}{k_n^{D-1}}\,\frac{\mathrm{d}n}{\mathrm{d}k_n}\right]_{k_n=p} = C\,\frac{A}{p^{D+1}}. \tag{31}$$

Now consider the probability density along any line in B, say, the x direction. Then the power spectrum of this function of x is

$$|a(k_x)|^2 = \int \mathrm{d}^D\boldsymbol{p}\,\delta(p_x - k_x)\left|\bar{\Psi}(\boldsymbol{p})\right|^2$$

$$\approx CA\int\frac{\mathrm{d}^{D-1}\boldsymbol{p}_\perp}{\left(k_x^2 + p_\perp^2\right)^{(D+1)/2}} \approx \frac{CA}{k_x^2}\int_0^\infty\frac{\mathrm{d}u\,u^{D-2}}{(u^2+1)^{(D+1)/2}} = \frac{CA}{k_x^2} \tag{32}$$

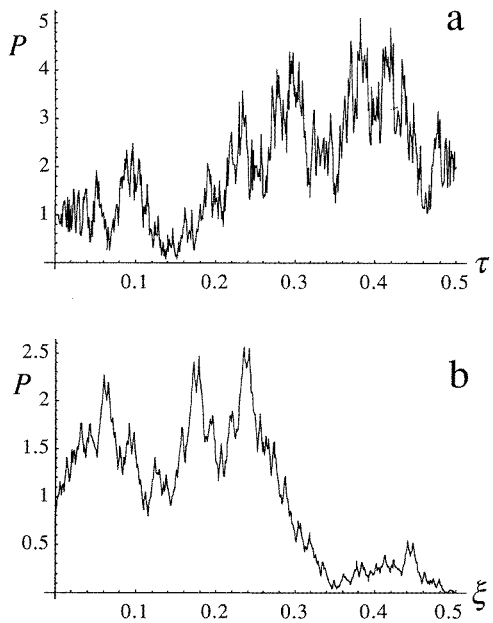

Figure 1. Probability density $P(\xi, \tau) = |\Psi(\xi, \tau)|^2$ for a particle in a one-dimensional box, calculated from (35). (*a*): as a function of τ for $\xi = 0$, showing the time fractal, with dimension $D_{\text{time}} = 7/4$. (*b*): as a function of ξ for $\tau = 1 - 2^{-1/3}$, showing the space fractal, with dimension $D_{\text{space}} = 3/2$.

where the last equality (with the constant C reassigned) is justified because the integral converges when $D \geqslant 2$ (and when $D = 1$ the power spectrum is given directly by (31)). Along this line, the fractal dimension D_{line} of the graph of P is given by (7), in which, from (6), $\beta = 2$. Thus

$$D_{\text{line}} = \tfrac{1}{2}(5 - 2) = \tfrac{3}{2}. \tag{33}$$

Finally, the fractal dimension of the hypersurface of P over $\boldsymbol{r}$ is (Mandelbrot 1982)

$$D_{\text{space}} = D_{\text{line}} + D - 1 = D + \tfrac{1}{2}. \tag{34}$$

4. One dimension

For a particle confined on the unit interval $|\xi| \leqslant 1/2$, the superposition (4) can be easily determined to be the following function of ξ and a rescaled time τ:

$$\begin{aligned}\Psi(\xi, \tau) &= \frac{2}{\pi} \sum_{n=0}^{\infty} \frac{(-1)^n}{\left(n + \frac{1}{2}\right)} \cos\left\{2\pi\, \xi \left(n + \tfrac{1}{2}\right)\right\} \exp\left\{-\mathrm{i}\pi\, \tau \left(n + \tfrac{1}{2}\right)^2\right\} \\ &= \frac{1}{\pi} \sum_{n=-\infty}^{\infty} \frac{(-1)^n}{\left(n + \frac{1}{2}\right)} \exp\left\{\mathrm{i}\pi \left[2\xi \left(n + \tfrac{1}{2}\right) - \tau \left(n + \tfrac{1}{2}\right)^2\right]\right\}\end{aligned} \tag{35}$$

(this formula is a special case of (20)–(23)). The symmetries

$$\begin{aligned}
&\Psi(\xi,-\tau)=\Psi^*(\xi,\tau)\,;\;\;\Psi(\xi,\tau+1)=\exp\{-\mathrm{i}\pi/4\}\;\Psi(\xi,\tau);\\
&\text{i.e. }\Psi(\xi,1-\tau)=\exp\{-\mathrm{i}\pi/4\}\,\Psi^*(\xi,\tau);\\
&\Psi(-\xi,\tau)=\Psi(\xi,\tau)\,;\;\;\Psi(\xi+1,\tau)=-\,\Psi(\xi,\tau);\\
&\text{i.e. }\Psi(1-\xi,\tau)=-\Psi(\xi,\tau)
\end{aligned} \tag{36}$$

mean that the probability density $P(\xi,\tau)$ need be calculated only for times $(0\leqslant\tau\leqslant 1/2)$, and can be periodically continued outside the box, that is for $|\xi|>1/2$. The wave (35), with a constant added, also describes the Talbot effect (Berry and Klein 1996) for light diffracted into the space $\tau>0$ beyond a grating with sharp slits whose width is half the grating period.

The series (35) converges slowly, but can still be used to compute Ψ and so illustrate the time and space fractals (figure 1 shows typical examples). The greater irregularity of the time fractal, with dimension $D_{\text{time}}=7/4$, in comparison with the space fractal, whose dimension (equation 34) is $D_{\text{space}}=3/2$, is evident, and the curves resemble others (e.g. Berry and Lewis 1980) with similar fractal dimensions. Both fractals are illustrated as a landscape in figure 2 (from the side) and figure 3 (in plan view). It appears that $P(\xi,\tau)$ is not an amorphous fractal, but contains much additional structure. Two aspects of this structure will now be elucidated.

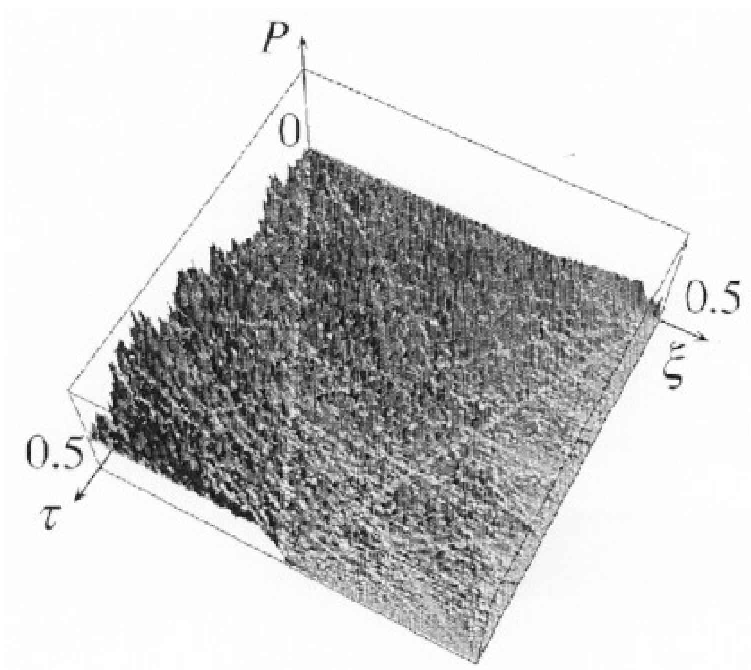

Figure 2. Illuminated landscape plot of the fractal probability density $P(\xi,\tau)$ in time and space for a particle in a box.

First, at rational times τ the graph of P is not fractal but is piecewise constant. For example, when $\tau=0$ the initial condition requires $P=1$, and when $\tau=1/2$ it can be seen in figures 2 and 3 that $P=2$ for $|\xi|<1/4$ and $P=0$ for $1/4\leqslant|\xi|<1/2$. These rational times correspond to *quantum revivals*, where the initial wave gets reconstructed by

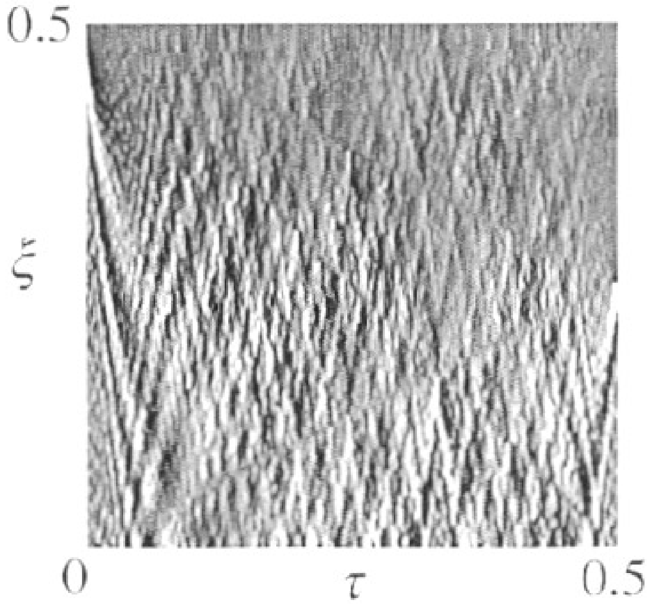

Figure 3. Plan view of the fractal probability density landscape $P(\xi, \tau)$ in time and space for a particle in a box.

constructive interference, either exactly (integer τ) or partially (τ fractional but non-integer). For a large class of quantum systems, the theory of revivals was given by Averbukh and Perelman (1989) and recently elaborated by Leichtle *et al* (1996) (see also Mallalieu and Stroud 1995). The particle in a box provides a surprisingly simple particular case that can be studied in detail; this fact was also appreciated by Stifter *et al* (1996), who gave the theory of revivals for this case and illustrated it with Gaussian (that is, smooth) wavepackets. The theory is almost identical to that of the self-images of diffraction gratings in the Talbot effect, given in detail elsewhere (see, for example, Berry and Klein 1996), so here I give just the outline of the analysis.

Let the wave (35) be written as the integral, over the initial state $\Psi(\xi, 0) = 1$, of the propagator $K(\xi, \tau)$, namely

$$\Psi(\xi,\tau) = \int_{-1/2}^{1/2} \mathrm{d}\xi_0 K\,(\xi - \xi_0, \tau)\,,$$
$$\text{where}\quad K(\xi,\tau) = \sum_{n=-\infty}^{\infty} \exp\left\{\mathrm{i}\pi\left[2\xi\left(n+\tfrac{1}{2}\right) - \tau\left(n+\tfrac{1}{2}\right)^2\right]\right\}. \qquad (37)$$

Now set $\tau = p/q$, where p and q are mutually prime integers, and split the sum into groups of q terms by defining

$$n = lq + s \qquad (-\infty < l < \infty,\ 1 \leqslant s \leqslant q). \qquad (38)$$

The crucial observation is that the exponential involving l^2 can be simplified, because

$$\exp\left\{-\mathrm{i}\pi pql^2\right\} = \exp\left\{-\mathrm{i}\pi q e_p l\right\} \qquad \text{where } e_p = 1\ (p \text{ even})\ 0\ (p \text{ odd}). \qquad (39)$$

This enables the sum over l to be evaluated as a series of δ functions, to give, after some reduction,

$$K\left(\xi,\frac{p}{q}\right)=\frac{1}{\sqrt{q}}\sum_{n=-\infty}^{\infty}A_n(q,p)\delta\left(\xi-\tfrac{1}{2}\left(e_p+\frac{p}{q}\right)-\frac{n}{q}\right)$$

where

$$A_n(q,p)=\frac{1}{\sqrt{q}}\exp\left\{\mathrm{i}\pi\left(\frac{p}{4q}+\frac{e_p}{2}+\frac{n}{q}\right)\right\}\times\sum_{s=1}^{q}\exp\left\{\mathrm{i}\frac{\pi}{q}\left((2n+qe_p)s-ps^2\right)\right\}. \quad (40)$$

When combined with the integral (37), this result shows that the wave for these rational times is the superposition of q shifted copies of the initial wave in the box (set equal to zero outside). The nature of the superposition is determined by the A_n, which are pure phase factors, that is

$$A_n(q,p)=\exp\{\mathrm{i}\Phi_n(q,p)\}. \quad (41)$$

The phases can be evaluated explicitly by recognizing the formula for A_n in (40) as a variant of the Gauss sum of number theory. An elementary derivation can be found in appendix A of Hannay and Berry (1980). The result is

$$\left.\begin{aligned}\Phi(n;q,p)&=\pi\left[\tfrac{1}{4}\left(q+\tfrac{p}{q}+1\right)+\tfrac{n}{q}+\tfrac{p}{q}(p\backslash q)^2n^2-\tfrac{1}{2}\begin{pmatrix}p\\q\end{pmatrix}\right] && (a)\\&=\pi\left[\tfrac{1}{4}\left(p+\tfrac{p}{q}\right)+\tfrac{n}{q}+\tfrac{p}{q}(p\backslash q)^2\left(n+\tfrac{1}{2}q\right)^2+1-\tfrac{1}{2}\begin{pmatrix}q\\p\end{pmatrix}\right] && (b)\\&=\pi\left[\tfrac{1}{4}\left(q+\tfrac{p}{q}+3\right)+\tfrac{n}{q}+\tfrac{4p}{q}(4p\backslash q)^2\left(n+\tfrac{1}{2}q\right)^2-\tfrac{1}{2}\begin{pmatrix}p\\q\end{pmatrix}\right] && (c)\end{aligned}\right\} \quad (42)$$

$(a):(p\text{ even},\ q\text{ odd})$; $(b):(p\text{ odd},\ q\text{ even})$; $(c):(p\text{ odd},\ q\text{ odd})$.

Here, $(p\backslash q)$ is the integer inverse of p mod q, given by

$$(p\backslash q)=p^{(\phi_E(q)-1)}\bmod q \quad (43)$$

where $\phi_E(q)$ denotes Euler's totient function (number of positive integers less than q that are relatively prime to q), and $\begin{pmatrix}p\\q\end{pmatrix}$ is the Jacobi symbol, which takes the value $+1$ or -1, and is defined as the product of Legendre symbols $\begin{pmatrix}p\\s\end{pmatrix}$ for all prime factors s of q, these in turn being defined as

$$\begin{pmatrix}p\\s\end{pmatrix}=\left.\begin{matrix}+1\text{ if there is an integer } m \text{ such that } m^2\equiv p \bmod s\\-1\text{ if there is no integer } m \text{ such that } m^2\equiv p \bmod s.\end{matrix}\right\} \quad (44)$$

Figure 4(a) shows an example of a fractional revival of the probability density, computed using these formulas. Confirmation of the correctness of the analysis was obtained by computing Ψ for the same τ with the modal series (35), which gave exactly the same picture (apart from Gibbs oscillations smoothing the discontinuities, caused by truncating the series).

The second peculiarity of the one-dimensional box was discovered after noticing the diagonal lines in figures 2 and 3. These lines correspond to particular spacetime slices through the P landscape, on which, as will now be shown, partial destructive interference between the terms in (35) reduces the fractal dimension.

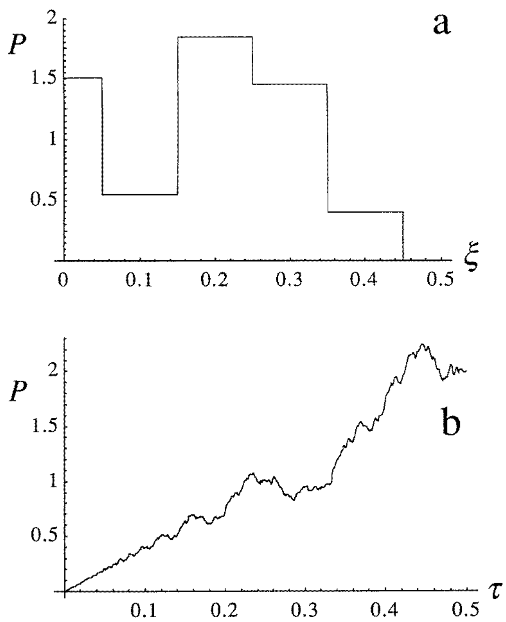

Figure 4. (a) Fractional quantum revival at time $\tau = 1/10$ for particle in one-dimensional box; (b) Fractal probability density along the spacetime slice $\xi = (1-\tau)/2$, with the dimension $D_{\mathrm{diagonal}} = 5/4$.

Consider the phase in the second sum in (35), namely

$$\chi(\xi, \tau, n) = \pi \left[n + 2\xi \left(n + \tfrac{1}{2} \right) - \tau \left(n + \tfrac{1}{2} \right)^2 \right] \tag{45}$$

on the spacetime slice

$$\xi = a\tau + \tfrac{1}{2}b. \tag{46}$$

We seek cancellation between pairs of exponentials with positive and negative n in (35), that is between n and $-n-k$. The condition for this is (after noting the opposite signs of the factor $1/(n+1/2)$ for positive and negative n),

$$\Delta\chi = 0 \ (mod\ 2\pi) \tag{47}$$

where

$$\begin{aligned} \Delta\chi &\equiv \chi\left(a\tau + \tfrac{1}{2}b, \tau, n\right) - \chi\left(a\tau + \tfrac{1}{2}b, \tau, -n-k\right) \\ &= \pi(2n+k)\left[1 + b + \tau(2a + k - 1)\right] \end{aligned} \tag{48}$$

The condition (47) must hold everywhere on the slice, that is for all τ, and also for all n. Thus

$$a = \tfrac{1}{2}(1-k), \qquad b \text{ integer.} \tag{49}$$

Therefore

$$\Delta\chi = \pi\, k(1+b) \tag{50}$$

from which follows, from (46),

$$b \text{ odd if } k \text{ is odd, } b \text{ unrestricted if } k \text{ is even.} \tag{51}$$

Collecting these results, we find cancellation on the lines

$$\xi = m\tau + n + \tfrac{1}{2} \quad (m \neq 0)\,, \qquad \xi = \left(m + \tfrac{1}{2}\right)\tau + \tfrac{1}{2}n \quad (m, n \text{ integer}). \tag{52}$$

Some of these lines are shown in figure 5. Note that the picture is not symmetrical; for example, the line $\xi = \tau$ is not present, although the line $\xi = 1/2 - \tau$ is. On any such line, the contribution of terms n, $-n-k$ in (35) is proportional to

$$\frac{1}{n+\frac{1}{2}} + \frac{1}{-n-k+\frac{1}{2}} = \frac{k-1}{\left(n+\frac{1}{2}\right)\left(n+k-\frac{1}{2}\right)} \to \frac{k-1}{n^2}. \tag{53}$$

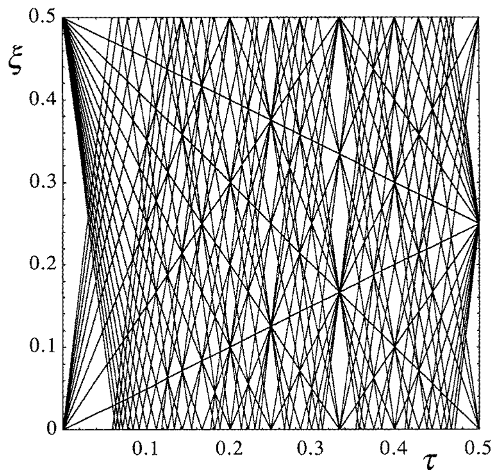

Figure 5. Spacetime lines on which the probability density for the particle in a one-dimensional box has the fractal dimension $D_{\text{diagonal}} = 5/4$.

In the power spectrum, the contribution of these terms is therefore reduced from n^{-2} to n^{-4}, giving an extra factor E^{-1} in the power spectrum (18) in the calculation of the time fractal. (The case $k = 1$ is an exception, because the cancellation is exact; this corresponds to the excluded value $m = 0$ in the first equation in (52), that is to the edges of the box, where $\Psi = 0$.) Therefore $\beta = 5/2$ in (6), and, from (7), the fractal dimension of the graph of P along these special spacetime lines is

$$D_{\text{diagonal}} = \tfrac{5}{4}. \tag{54}$$

One of these diagonal fractals is shown in figure 4(*b*); it is noticeably less irregular than either of the fractals in figure 1, whose fractal dimensions are greater. Duistermaat (1991) gives a full analysis of a function closely related to this 'diagonal' special case. The lines (52) also appear as 'canals' in the analogous computations for Gaussian wavepackets (Stifter *et al* 1996).

There may be further treasures hidden in the sum (35), for example spacetime lines (not necessarily straight) on which more complicated interference between groups of terms leads to fractal probability densities with dimensions different from D_{time}, D_{space}, or D_{diagonal}.

5. Fractals in fractal boxes

Suppose now that the box has a fractal boundary, that is ∂B has dimension $D - 1 + \gamma$ (where $0 \leqslant \gamma < 1$), rather than $D - 1$. Therefore the area A (that is, the $D - 1$ measure of ∂B) is infinite, but the $D-1+\gamma$ measure A_γ is finite. The arguments of sections 2 and 3 no longer apply, because they lead to divergent formulae involving A (cf (18) and (32)). I will suggest a simple modification that gives D_{time} and D_{space} in these cases. The modification is the same as that which led to a modified form of the corrections to Weyl's law for the eigenvalue counting function in boxes with fractal boundaries (Berry 1979); this was far from rigorous, and it is still not clear exactly when it applies (see e.g. Lapidus 1991, Lapidus and Pomerance 1996), although it probably holds for 'non-pathological fractals', where the Hausdorff, Minkowski and other fractal dimensions of ∂B are the same.

The physical idea underlying the modification is that the box eigenfunction $\phi_n(\boldsymbol{r})$ is insensitive to details of ∂B on linear scales finer than the wavelength $1/k_n$. This suggests that in calculating the mode coefficient c_n in (4), ∂B can be replaced by the boundary smoothed over a wavelength, so that A can be replaced by the wavelength-smoothed area $A(k_n)$, where

$$A(k) \approx A_\gamma k^\gamma . \tag{55}$$

With this replacement, and recalling $k=\sqrt{E}$, the power spectrum (18) becomes

$$|a(E)|^2 = \frac{C\,A_\gamma}{V\,E^{(3-\gamma)/2}} . \tag{56}$$

Thus in (7) β acquires an extra contribution $-\gamma/2$, and the dimension of the time fractal is changed from (19) to

$$D_{\text{time}} = \frac{(7+\gamma)}{4} . \tag{57}$$

Similar reasoning applied to (31) gives an extra factor k^γ in (31), and hence an extra factor k_x^γ in (32), so that now β acquires an extra contribution $-\gamma$, and the dimension of the space fractal is changed from (34) to

$$D_{\text{space}} = D + \frac{1}{2} + \frac{\gamma}{2} . \tag{58}$$

It is interesting that in the limit $\gamma \to 1$ for which ∂B is no longer continuous, the probability density P approaches a function that is discontinuous in both time (because $D_{\text{time}} \to 2$) and space (because $D_{\text{space}} \to D+1$).

Acknowledgments

I thank Dr J H Hannay and Dr J P Keating for helpful suggestions, and Professor W P Schleich for showing me a draft of his paper on quantum revivals (Stifter *et al* 1996).

Appendix. Intensity and amplitude fractals

For the amplitude (5), the intensity is

$$I(u) \equiv |f(u)|^2 = \sum_m \sum_n a_m a_n^* \exp\{\mathrm{i}(m-n)\,u\} \equiv \sum_l I_l \exp\{\mathrm{i}l\,u\} ,$$
$$\text{where } I_l = \sum_n a_{n+l} a_n^* . \tag{A1}$$

The power spectrum of $I(u)$ is the average of $|I_l|^2$ over the random phases of the a_m, that is

$$\langle |I_l|^2 \rangle_{\text{phases}} = \left\langle \sum_m \sum_n a_{m+l}^* a_{n+l} a_m a_n^* \right\rangle_{\text{phases}} = \sum_n |a_{n+l}|^2\,|a_n|^2 . \tag{A2}$$

For $|l| \gg 1$, the sum over n is dominated by the regions near $n = 0$ and $n = -l$, and the asymptotic behaviour (6) gives

$$\left\langle |I_l|^2 \right\rangle_{\text{phases}} \propto \frac{2}{|l|^\beta} \sum_n |a_n|^2. \tag{A3}$$

The sum exists whenever $\beta > 1$, that is whenever the function $f(u)$ is continuous. Then the power spectrum of the intensity I, and hence its fractal dimension, is indeed the same as that of Re f and Im f, as argued in section 1.

References

Averbukh I Sh and Perelman N F 1989 *Phys. Lett.* **39A** 449–53

Baltes H P and Hilf E R 1976 *Spectra of Finite Systems* (B-I Wissenschaftsverlag: Mannheim)

Berry M V 1977 *J. Phys. A: Math. Gen.* **10** 2083–91

Berry M V 1979 Distribution of modes in fractal resonators *Structural Stability in Physics* eds W Güttinger and H Eikemeier (Berlin: Springer) 51–3

Berry M V and Klein S 1996 *J. Mod. Opt.* in press

Berry M V and Lewis Z V 1980 *Proc. R. Soc.* A **370** 459–84

Duistermaat J J 1991 *Nieuw Arch. voor Wis.* **9** 303–37

Hannay J H and Berry M V 1980 *Physica* **1D** 267–90

Lapidus M L 1991 *Trans. Amer. Math. Soc.* **325** 465–529

Lapidus M L and Pomerance C 1996 *Math. Proc. Camb. Phil. Soc.* **119** 167–78

Leichtle C, Averbukh I Sh and Schleich W P 1996 Generic structure of multilevel quantum beats *Preprint* University of Ulm

Mallalieu M and Stroud C R Jr 1995 *Phys. Rev.* A **51** 1827–35

Mandelbrot B B 1982 *The Fractal Geometry of Nature* (Freeman: San Francisco)

Orey S 1970 *Z. Warsch. verw. Geb.* **15** 249–56

Stifter P, Leichtle C, Lamb W E and Schleich W P 1996 in preparation